UAN-Engineering Test: P2P Communications

U. Vilaipornsawai and A. Silva

University of Algarve   tel: +351-289244422
Campus de Gambelas   fax: +351-289864258
8005-139, Faro   cintal@ualg.pt
Portugal   www.cintal.ualg.pt

Work requested by	CINTAL
	Universidade do Algarve, Campus de Gambelas,
	8005-139 Faro, Portugal
	tel: +351-289244422, cintal@ualg.pt,
	www.cintal.ualg.pt
Laboratory performing	Signal Processing Laboratory (SiPLAB)
the work	Universidade do Algarve, Campus de Gambelas,
	8005-139 Faro, Portugal
	tel: +351-289800949
Project	UAN-Underwater Acoustic Network:Contract FP7
Title	UAN-Engineering Test: P2P Communications
Authors	U. Vilaipornsawai, A. Silva, and S.M. Jesus
Date	December 15, 2010
Reference	05/10 - SiPLAB
Number of pages	37 (thirty-seven)
Abstract	This report describes the P2P communication setup and results from the engineering test conducted at Pianosa island, Italy during September 7-25, 2010.
Clearance level	CINTAL, ISME, FOI, Kongsberg Maritime,SINTEF, SSI
Distribution list	CINTAL,ISME, FOI, Kongsberg Maritime,SINTEF, SSI

Approved for publication

Sérgio Jesus

President Administration Board

Contents

List of Figures

Chapter 1

Point to Point (P2P) Communications

1.1 Introduction

This report presents the experiment set up and results for the Point to Point (P2P) communications in the Underwater Acoustic Network (UAN) engineering test, conducted on Pianosa island, Italy during Sept 7-25, 2010. The objectives of P2P communication experiments are

1. To perform high data rate and reliable communications between an acoustic source and a Vertical Line Array (VLA) of hydrophones for multi-channel reception, providing spatial diversity.

2. To investigate the performance of the currently developed data processing techniques and to further improve such techniques.

   This document is organized as follows: first the location and the precise positions of source and the VLA are presented, and the system setup including the mooring information of the VLA is discussed, followed by the discussion of the transmitted signal descriptions. Then, the signal process based on the pTR and Frequency-shifted pTR (FSpTR) [1] combined with an equalizer as well as MultiChannel equalizer (MC-E) are presented. Finally, the conclusions are drawn.

1.2 P2P communication setup

Throughout this report, latitude and longitude coordinates in degrees and decimals, and GMT time are used.

   In P2P communications, acoustic signals were generated by Portable Acoustic Source Unit (PASU) (refer to [2] for detailed descriptions) and transmitted by a Lubell acoustic source to a VLA of hydrophones. The VLA was connected to the Subsurface Telemetry Unit (STU) [2] that acquires multiple received signals. Then, the signals were sent to a

shore lab via a fiber optic cable for data processing to recover the transmitted information. This system is considered as a Single Input Multiple Output (SIMO) communication system.

Various P2P configurations were conducted in this experiment by changing the locations of the source, while fixing the VLA. Three P2P configurations were carried on, with the source transmitting signals generated from PASU placed at 1. the pier of the Pianosa island, 2. on a rubber boat and 3. from Leonardo research vessel at four fixed stations, denoted by S1 to S4.

On September 10, 2010, the STU along with the VLA of 16 hydrophones and a Kongsberg Maritime (KM) underwater acoustic modem and a 1km fiber optic and power cables were connected to the shore lab. Hereafter, the 16-channel VLA is referred to as VLA16 and its mooring is shown later in Figure 1.3. For P2P communications from pier and rubber boat, the VLA16 was used. During the experiment, due to a thunder storm on Sept 13, 2010, there was water leakage into the array connectors and the STU, damaging one of the two acquisition boards (with 12 channels each). This resulted in only 12 channels available. On Sept 20, 2010, a spared VLA of 8 hydrophones, referred to as VLA8, was deployed, and the P2P communications between the source at S1-S4 with this VLA were conducted. The mooring of the VLA8 is shown in Figure 1.4.

Figure 1.1 illustrates the bathymetry of the area where P2P communications took place, using data from multibeam bathymetric survey. The blue '+' marks the VLA16 position at 42.5924° N and 10.1084° E with water column depth of about 56.6m. The blue 'x' marks the pier at Pianosa island where the stationary acoustic source with signal generated from PASU was placed at position 42.5893° N and 10.0991° E round 1m below the sea surface at water column of around 2m. The distance between the stationary source and the VLA is around 836m. Moreover, the P2P communications were conducted by placing the acoustic source from the rubber boat at depth around 11m below the surface with its track shown by multi-color lines and discussed in more details later in the report. Furthermore, the source was placed from Leonardo at depth around 9m from the surface on range dependent track at positions S1 to S4 as shown in Figure 1.1 by magenta '∗' marks.

Table 1.1 summarizes the latitude and longitude coordinates of VLAs with VLA16 and VLA8 denote the VLA locations for the first and second deployments (within 20m apart). The locations of the pier and S1-S4 as well as their distance from the VLA are also presented in Table 1.1. Note that the distances calculated for pier and boat cases are with respect to VLA16, while those for S1-S4 cases are with respect to VLA8.

Table 1.1: Positions of VLAs, Pier, and S1 to S4

Case	Latitude	Longitude	Distance from VLA (m)
VLA16	42.5924° N	10.1084° E	-
VLA8	42.5922° N	10.1086° E	-
Pier	42.5893° N	10.0991° E	836
Boat	varied	varied	50-600
S1	42.5940° N	10.1060° E	292
S2	42.5933° N	10.1051° E	312
S3	42.5926° N	10.1036° E	412
S4	42.5915° N	10.1024° E	513
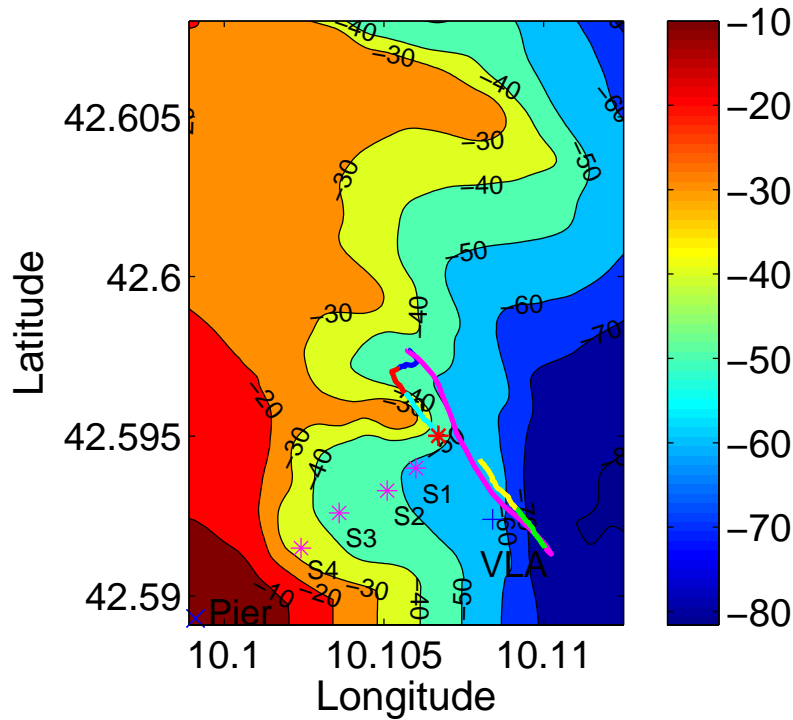
Figure 1.1: P2P communication area with VLA and source positions

Figure 1.2 illustrates the deployment of the Lubell acoustic source and KM modem from the rubber boat. The source and modem were placed at 11m and 16m, respectively, below the surface.

Figure 1.3 illustrates the mooring setup for the 16-hydrophone VLA at position VLA16 in Table 1.1 with water column depth of 56.6m. In this Figure, the dimensions of the setting are indicated to facilitate the association between channel characteristics observed at different hydrophones with depth-dependent sound speed profile. The VLA consists of 16 hydrophones, with spacing of approximately 2m. Note that since the original 4m-spacing array was folded to allow hydrophone spacing of 2m, the hydrophones were ordered as follows: 16, 1, 15, 2, 14, 3, 13, 4, 12, 5, 11, 6, 10, 7, 9, 8, from bottom to top, respectively.

The second mooring of the 8-hydrophone VLA at position VLA8 in Table 1.1 at water column of 58.3m is shown in Figure 1.4. The array was folded and the hydrophones 7, 1, 6, 8, 2, 5, 3, 4, were ordered from bottom to top, respectively.

KM PC

PASU PC

Sea surface

11m

Lubell acoustic source

5m
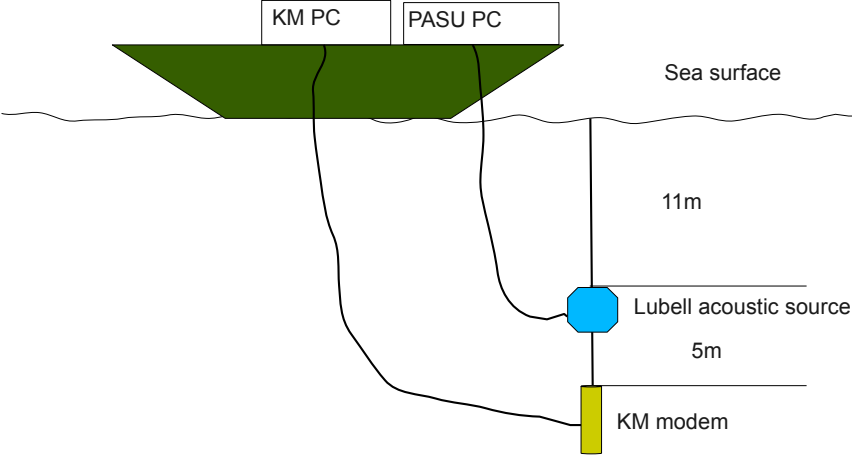
KM modem

Figure 1.2: Acoustic source and KM modem deployment from a rubber boat.
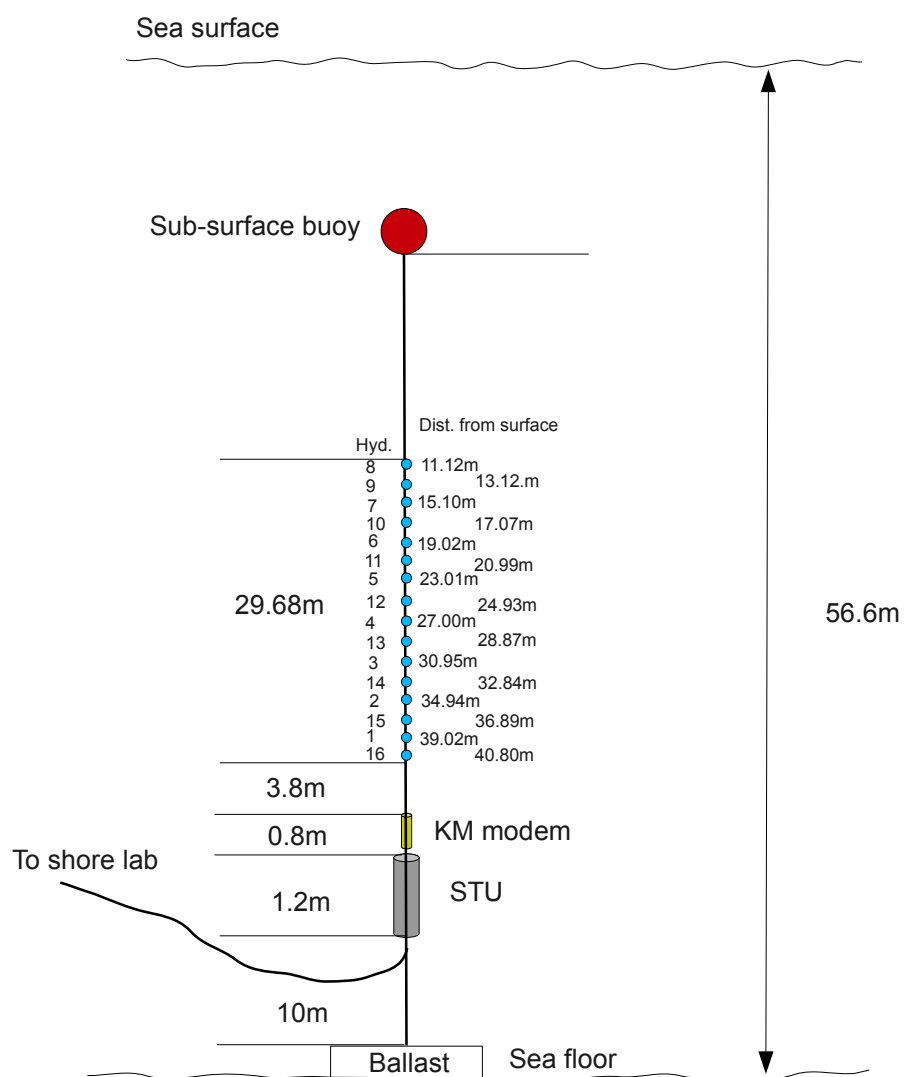
Figure 1.3: The 16-hydrophane VLA mooring at position VLA16.

Sea surface

Sub-surface buoy

Dist. from surface

Hyd.

4	30.9m
3	34.3m
5	35.9m
2	37.5m
8	39.4m
6	40.85m
1	42.35m
7	44.30m

13.40m

58.3m

7m

0.8m   KM modem

To shore lab

1.2m   STU

5m

Ballast   Sea floor

Figure 1.4: The 8-hydrophane VLA mooring at position VLA8.

1.3   Transmitted signal descriptions

Table 1.2 presents the signal codes and descriptions of signals sent during P2P communications, where Ai, i=1,2,...,22 denotes a tone signal with frequency i kHz and Bi, i=1,2,...,6, for chirp signals within 1 to 22 kHz band. The signal codes Ci for i=1,2,3,4 denote the BPSK modulated signals with carrier frequencies, f_c of 5, 10, 15 and 19.6 kHz, and transmission rates of 600, 1200, 2400, and 4800 symb/s, respectively. We use the fourth-root raised cosine shaping pulse with an excess bandwidth of 50%, hence the bandwidths of C1 to C4 signals are 0.9, 1.8, 3.6 and 7.2[1] kHz, respectively. ISME denotes the spread spectrum signal prepared by ISME, and FOI denote M-QAM modulated signal of turbo coded data that will be discussed in more details in separate documents. The QPSK modulated si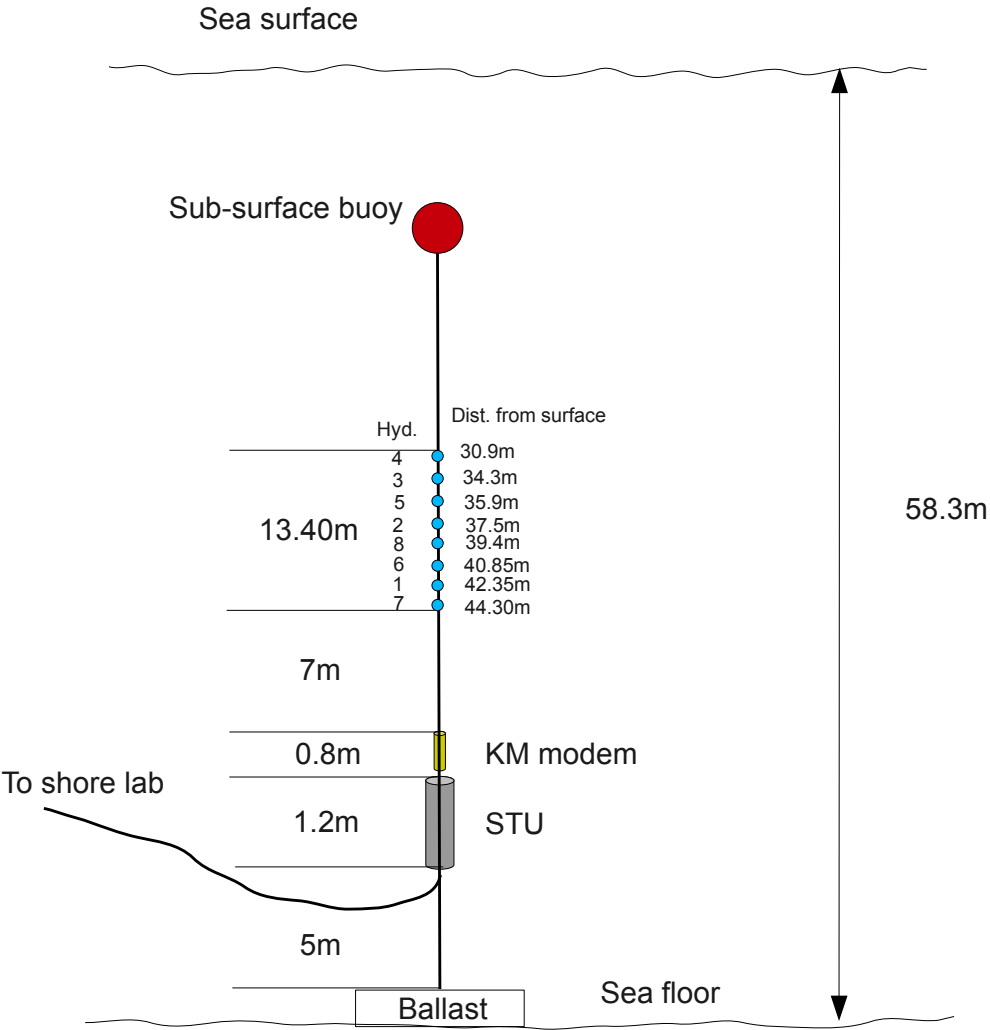gnal with $f_c = 25.6$ kHz with data rate of 2000 symb/s was transmitted from the KM modem and named as Transparent Signal (TsP). Despite a brief description of the TsP signal in this report, a more elaborate details will be presented in a separate document.

Table 1.2: Signal codes used in the engineering test at Pianosa island

Code	Type	Duration T (s)	Carrier Freq. f_c (kHz)	Baud Rate (symb/s)	Start-Stop Freq. (kHz)	Bandwidth (kHz)
A1	Tone	0.1	-	-	1-1	-
A2	Tone	0.1	-	-	2-2	-
⋮	⋮	⋮	⋮	⋮	⋮	⋮
A22	Tone	0.1	-	-	22-22	-
B1	Chirp	0.2	-	-	1-4	3
B2	Chirp	0.2	-	-	4-8	4
B3	Chirp	0.2	-	-	8-12	4
B4	Chirp	0.2	-	-	12-16	4
B5	Chirp	0.2	-	-	16-20	4
B6	Chirp	0.2	-	-	20-22	2
C1	BPSK	20	5	600	4.55-5.45	0.9
C2	BPSK	20	10	1200	9.1-10.9	1.8
C3	BPSK	20	15	2400	13.2-16.8	3.6
C4	BPSK	20	19.6	4800	16-23.2	7.2
TpS	QPSK	25	25.6	2000	24.1-27.1	3

The detailed structure of C1-C4 are presented in Table 1.3, where a sequence of M-sequence followed by information data together with duration of 1s is repeated for 20 times to constructure Ci signal with total duration of 20s.

Table 1.4 presents the detailed structure of TpS signal, which consists of 4 M-sequences each with length 127 symbols as preamble and preamble signals. The payload data has 25s duration, with each second includes an M-sequence and 1873 symbols (for a total of 2000 symb/s).

---

[1]However, due to the limitation of the PASU system with maximum sampling frequency of 44.1 kHz, only signals with frequency upto 22.05 kHz can be transmitted, resulting in the cut in the upper excess bandwidth of C4.

Table 1.3: Structure of C1-C4 signals

Type	M-seq	Data	$\cdots$	M-seq	Data
C1	63symb	537symb	repeated 18 times	63symb	537symb
C2	127symb	1073symb	repeated 18 times	127symb	1073symb
C3	255symb	2145symb	repeated 18 times	255symb	2145symb
C4	511symb	4289symb	repeated 18 times	511symb	4289symb

Table 1.4: Structure of TpS signal

Preamble	M-seq	Data	$\cdots$	M-seq	Data	Postamble
508symb	127symb	1873symb	repeated 23 times	127symb	1873symb	508 symb

The signals in Table 1.2 are transmitted in a sequence as presented in Table 1.5 as well as signals from ISME and FOI, having the total duration of 4:30 minutes. Chirp signals, B1-B6 were used to separate different sets of signals.

Table 1.5: PASU P2P transmitted signal sequence

A1-A22	B1-B6	C1	B1-B6	C2	B1-B6	C3	B1-B6	C4	B1-B6	ISME	B1-B6	FOI	B1-B6

1.4   At-sea Test

In this UAN2010 sea trial, three P2P configurations were conducted with their details given in the followings.

1.4.1   At Pianosa pier

On Saturday, September 11, 2010 (Julian day 254), at around 20:00 GMT (22.00 local time), the pier P2P communication was performed, where the source generated from PASU was placed at the pier as shown in Figure 1.1 by blue 'x'. Four batches of data were transmitted and the duration of the transmission was about 18 min. The starting time of each signal batch can be determined from raw data filenames, with details given in Appendix A and Table 2.1.

1.4.2   At-sea test from a rubber boat

On Monday, September 13, 2010 (Julian day 256), at around 7:36 GMT (9:36 local time), the rubber boat P2P communication was conducted, where the Lubell acoustic source and KM modem were placed from a rubber boat as shown in Figure 1.2. Moreover, the PASU and KM PC were also placed on board the boat with source depth of around 11m from the surface as shown in Figure 1.5. Note that source depths were obtained from
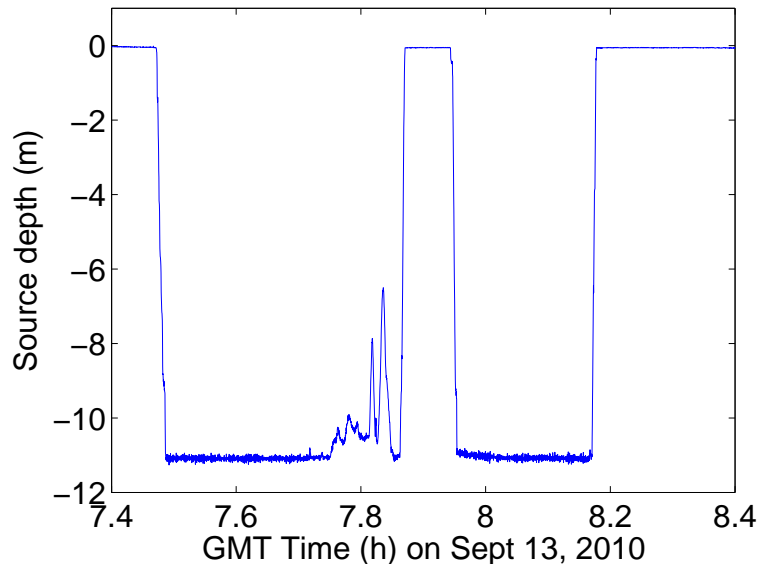
Figure 1.5: Source depth (m) measured from a pressure sensor on September 13, 2010 during the rubber boat P2P transmissions

the pressure recorded continuously in time during both data transmissions and transition periods, where the depths were around 11m and 0m, respectively. Source depths shown in Figure 1.5 can be associated with transmission frames presented in Appendix A.

In Figure 1.1, the track of a rubber boat is also shown. The red '∗' marks the beginning of the track where the signals was transmitted. Four batches of signals were transmitted during 33:30 minutes transmission (with some silence periods) and the starting transmission times can be found in Table 2.1 in Appendix A. The track along the isobathymatry is divided in six sections of an equal time duration using different color codes. From the figure we observe that in the fourth portion, there are stronger movement shown by a larger displacement during this section. This observation corresponds well with the velocity of the boat during the transmission, calculated by the displacement of the boat based on GPS data as shown in Figure 1.6. Figure 1.7 illustrates the distance between source and the VLA during the P2P transmissions, where the distances approaching 50-600 m are obtained.
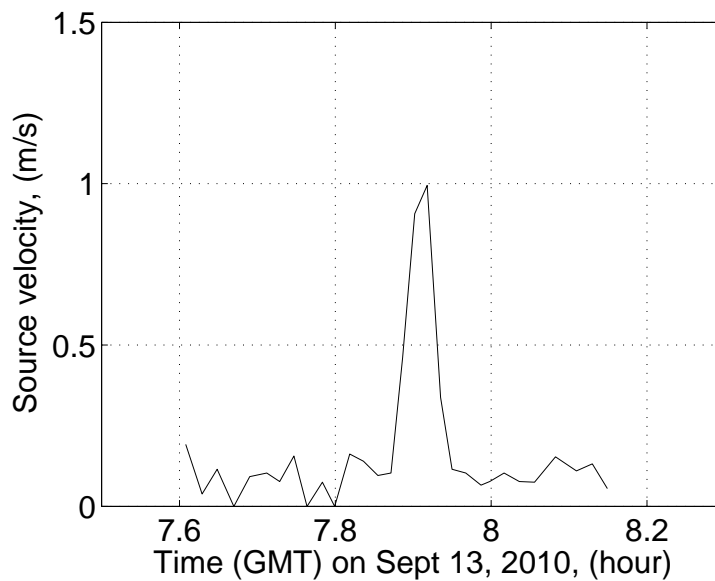

Figure 1.6: Rubber boat (source) velocity (m/s), estimated from GPS information

1.4.3 At-sea test from Leonardo research vessel

On Monday, September 20, 2010 (Julian day 263), at around 12:29 GMT (14:29 local time) the acoustic source with signal generated from PASU was placed from Leonardo at positions S1-S4 as shown in Figure 1.1 and presented in Table 1.1. The positions of S1-S4 are along a range-dependent track. Six batches of signals were transmitted and the starting transmission times can be found in Table 2.1 in Appendix A. The source was placed at approximately 9m depth from the surface as shown in Figure 1.8.
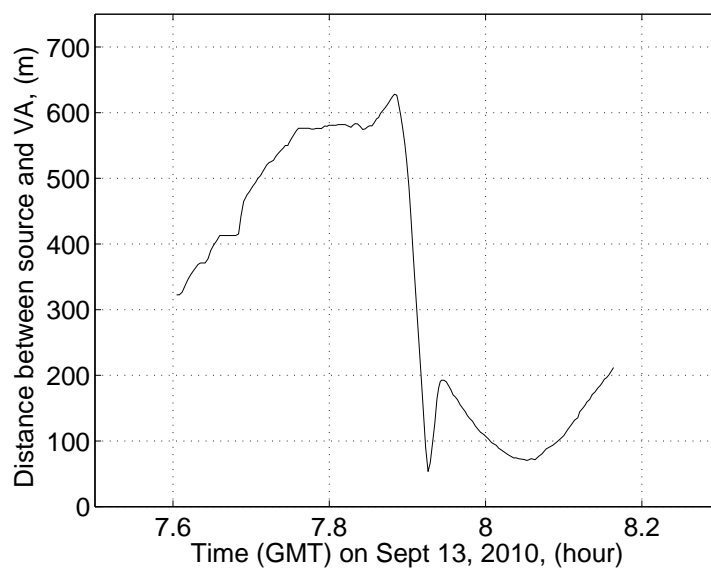
Figure 1.7: Rubber boat (source) distance from VLA16 (m), estimated from GPS information
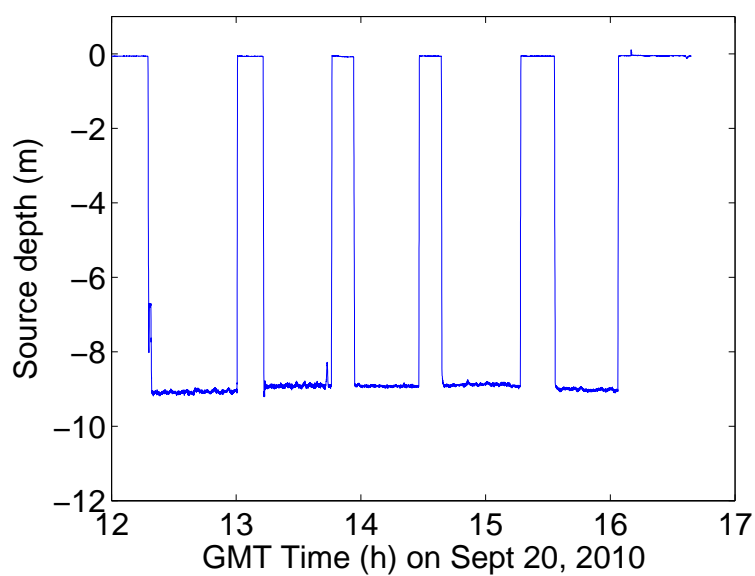

Figure 1.8: Source depth (m) measured from a pressure sensor on September 20, 2010 during S1-S4 P2P transmissions

1.4.4 Sound Speed Profile (SSP)

Using Conductivity Temperature and Depth (CTD) profiler, the sound speed profiles of the experiment area were recorded between September 12-28, 2010. Figure 1.9 presents the SSPs for September 12-17, 2010, covering the time that the VLA16 was deployed. For September 20-28 where the VLA8 was deployed, 2010, the SSPs are presented in Figure 1.10. The VLA16 and VLA8 positions are also presented in Figures 1.9 and 1.10, respectively for references.

(a) SSP for September 12, 2010   (b) SSP for September 13, 2010
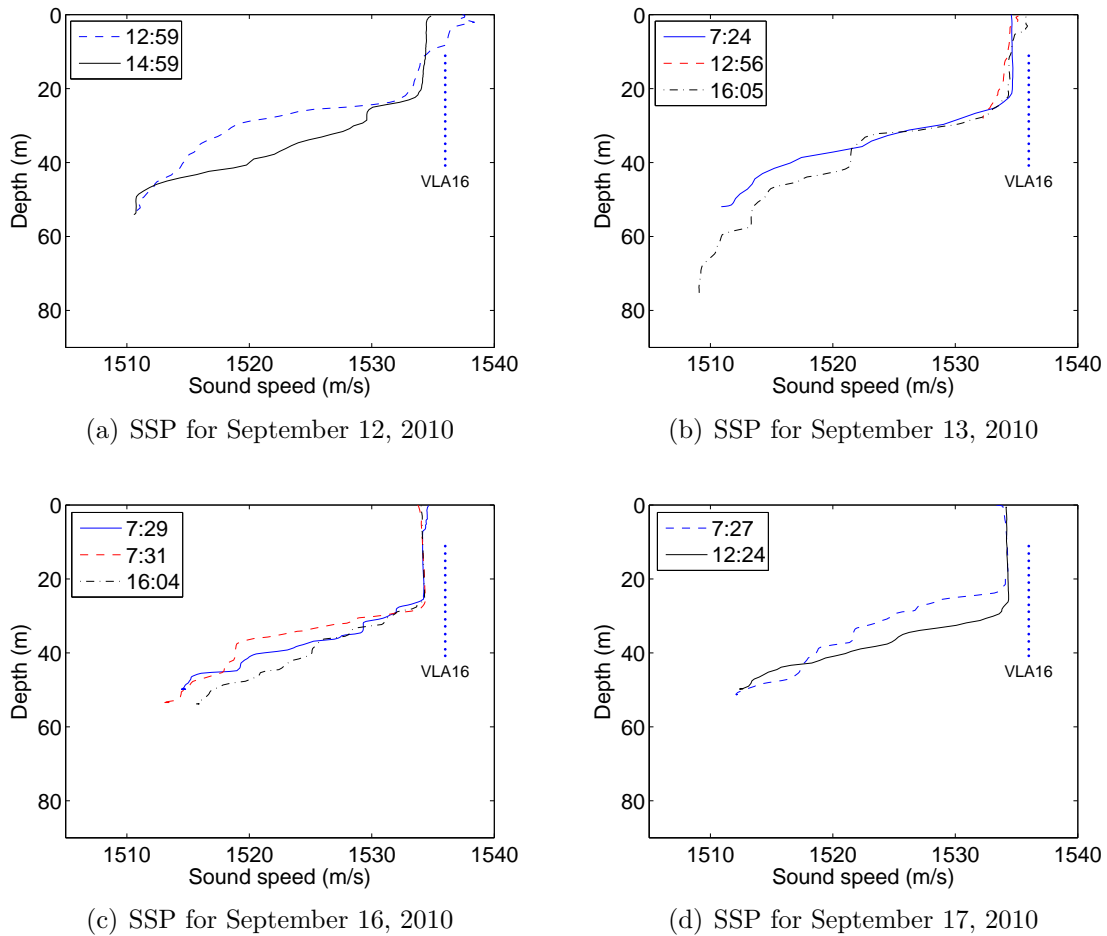
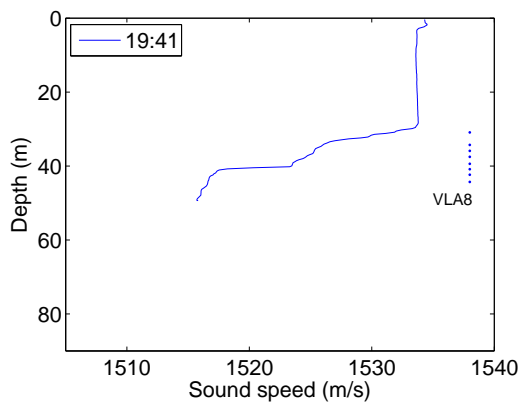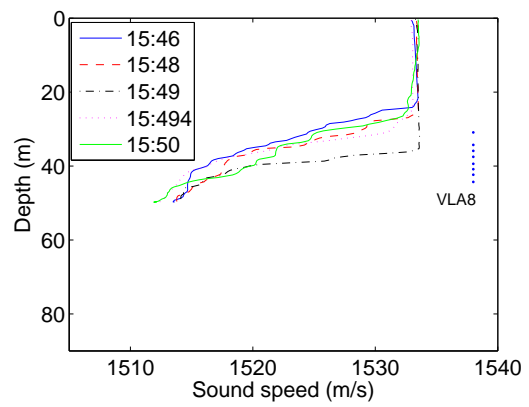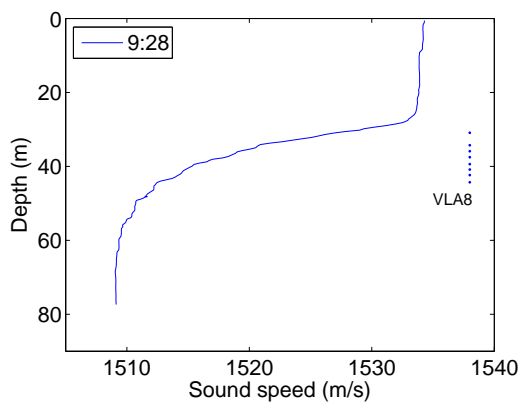(c) SSP for September 16, 2010   (d) SSP for September 17, 2010

Figure 1.9: Sound speed profiles between September 12-17, 2010

(a) SSP for September 20, 2010

(b) SSP for September 22, 2010

(c) SSP for September 23, 2010
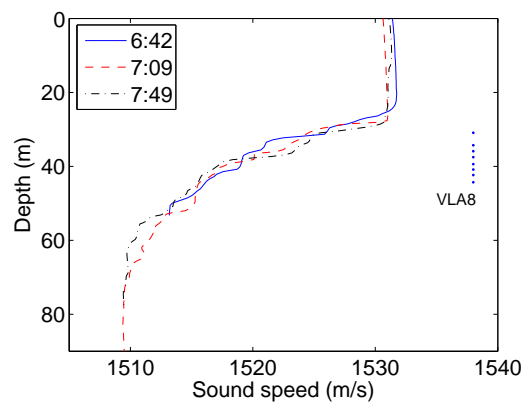
(d) SSP for September 28, 2010

Figure 1.10: Sound speed profiles between September 20-28, 2010

1.5 Signal Analysis

This section presents the spectrograms of transmitted and received signals, the channel frequency response estimated from chirp signals, as well as the Mean Square Error (MSE) and Bit Error Rate (BER) performance of the pTR-E and FSpTR-E and MC-E techniques.

1.5.1 Transmitted signals

Figure 1.11 shows the spectrogram of the transmitted signal sequence, which includes tones, chirp signals, C1-C4, ISME and FOI signals. The frequency bands of each signal correspond to the information given in Table 1.2. Note that there is a cut in frequency of the C4 signal, due to insufficient sampling frequency of 44.1 kHz generated by PASU which can not support a frequency band beyond 22.05 kHz, while the frequency band of C4 is 16-23.2 kHz.
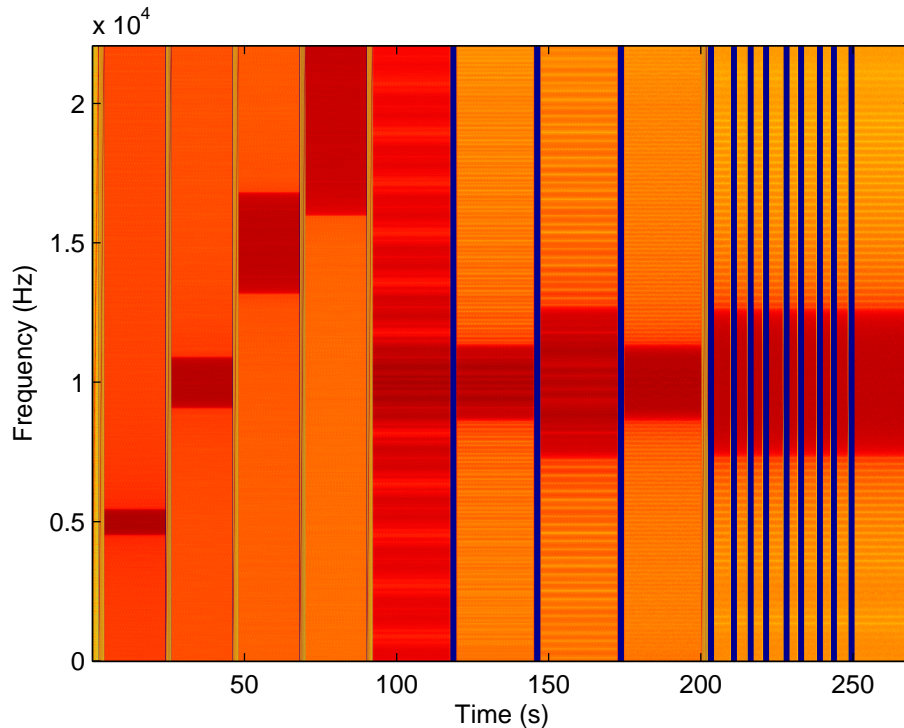
Figure 1.11: Spectrogram of a batch of transmitted signals.

Figure 1.12 presents zoom-in transmitted tone signals, A1-A22, where the descriptions of A1-A22 are given in Table 1.2.

The spectrogram of transmitted chirp signals, B1-B6 with their descriptions given in Table 1.2 is shown in Figure 1.13.
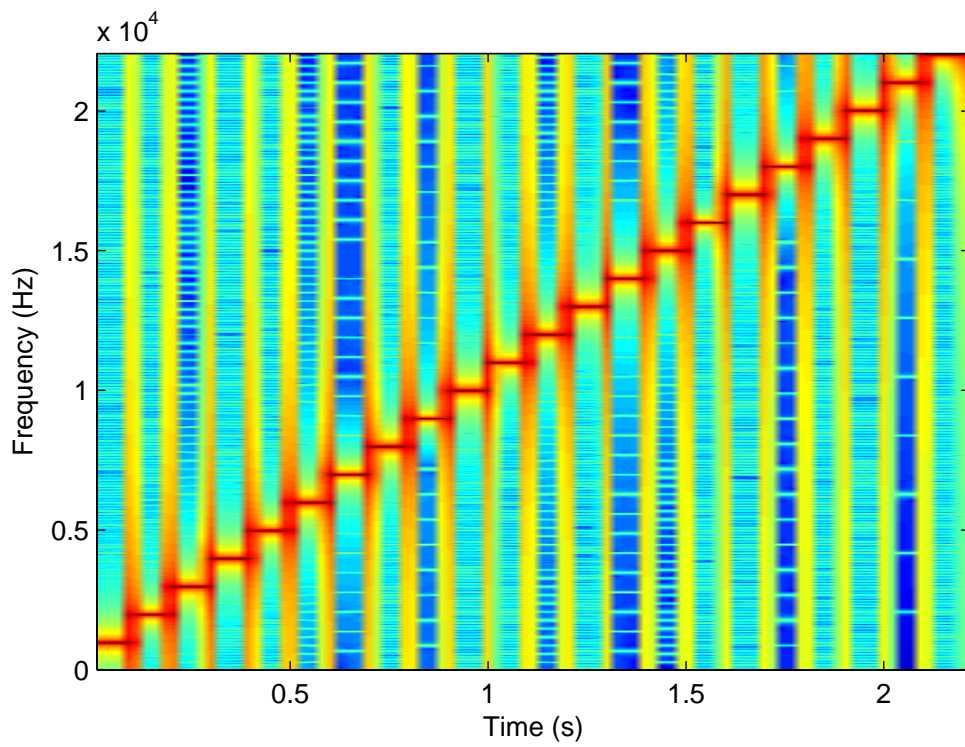
Figure 1.12: Spectrogram of transmitted tone signals A1-A22.
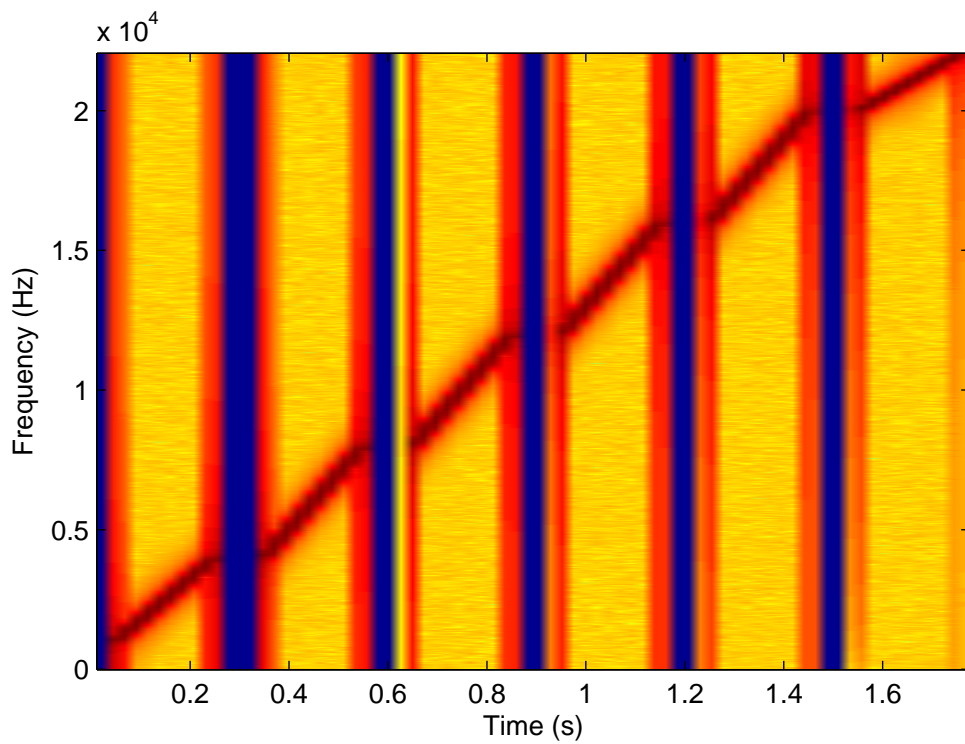
Figure 1.13: Spectrogram of transmitted chirp signals B1-B6.

1.5.2 Received signals

Figure 1.14 shows the spectrogram of the received signal sequence, which includes tones, chirp signals, C1-C4, ISME and FOI signals. The frequency bands of each signal correspond to those of transmitted signal shown in Figure 1.11 and the detailed information is given in Table 1.2.
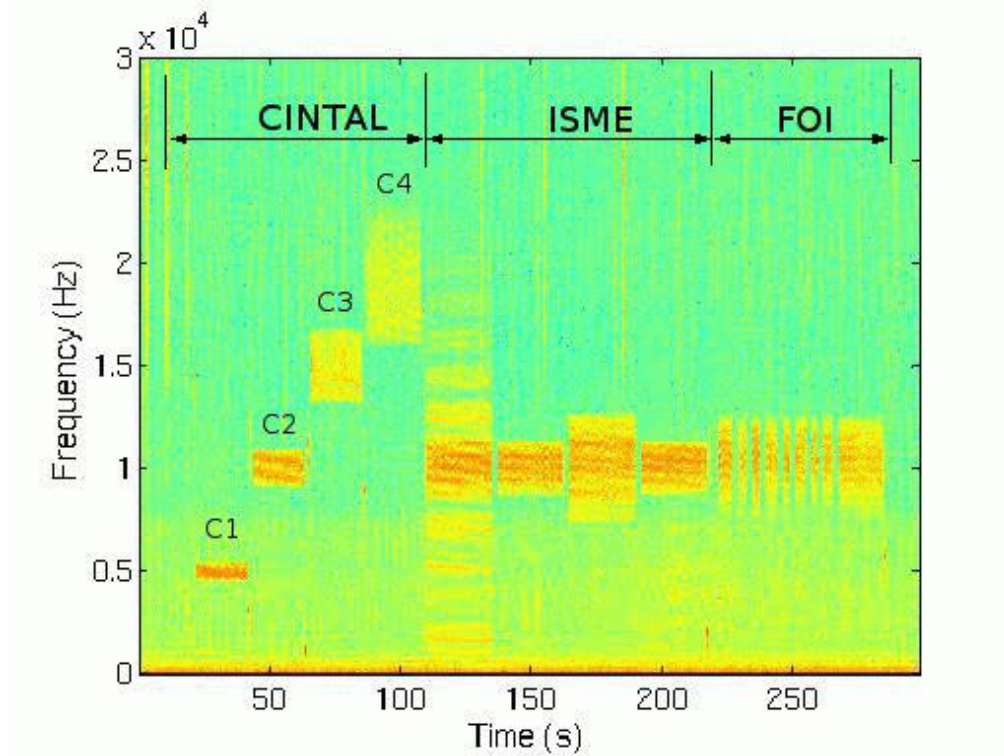
Figure 1.14: Spectrogram of a batch of received signals from the 8th hydrophone (depth 11.12m) of the VLA16.

Figure 1.15 illustrates received tone signals, A1-A22, where their descriptions can be found in Table 1.2.

The spectrogram of received chirp signals, B1-B6 is shown in Figure 1.16, where the detailed descriptions of the signals are given in Table 1.2.
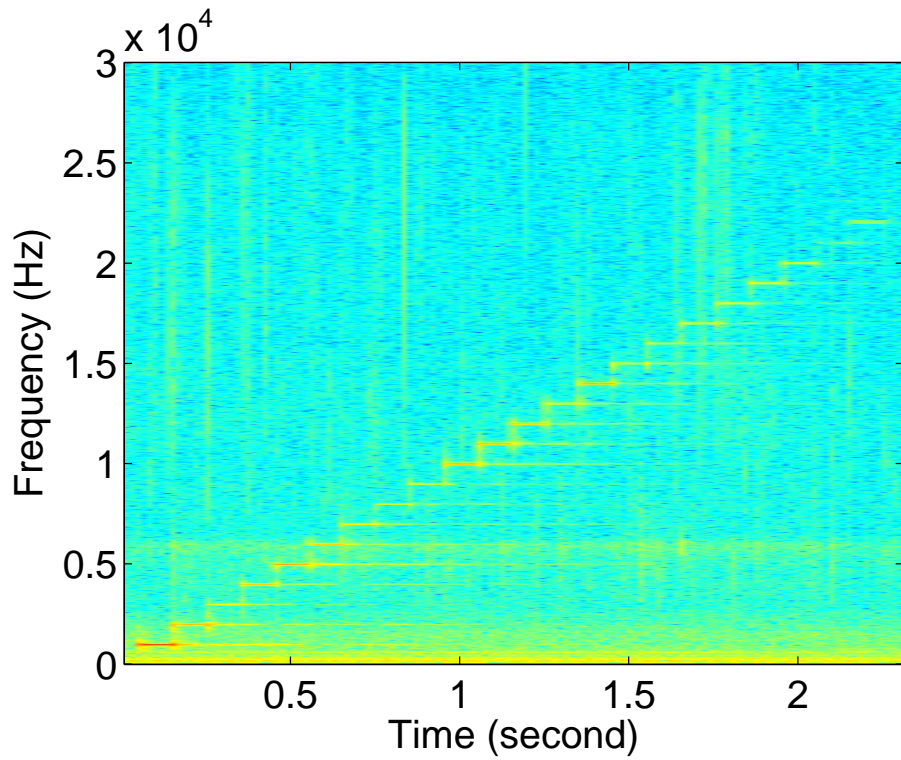
Figure 1.15: Spectrogram of received tone signals A1-A22 from the 8th hydrophone (depth 11.12m) of the VLA16.
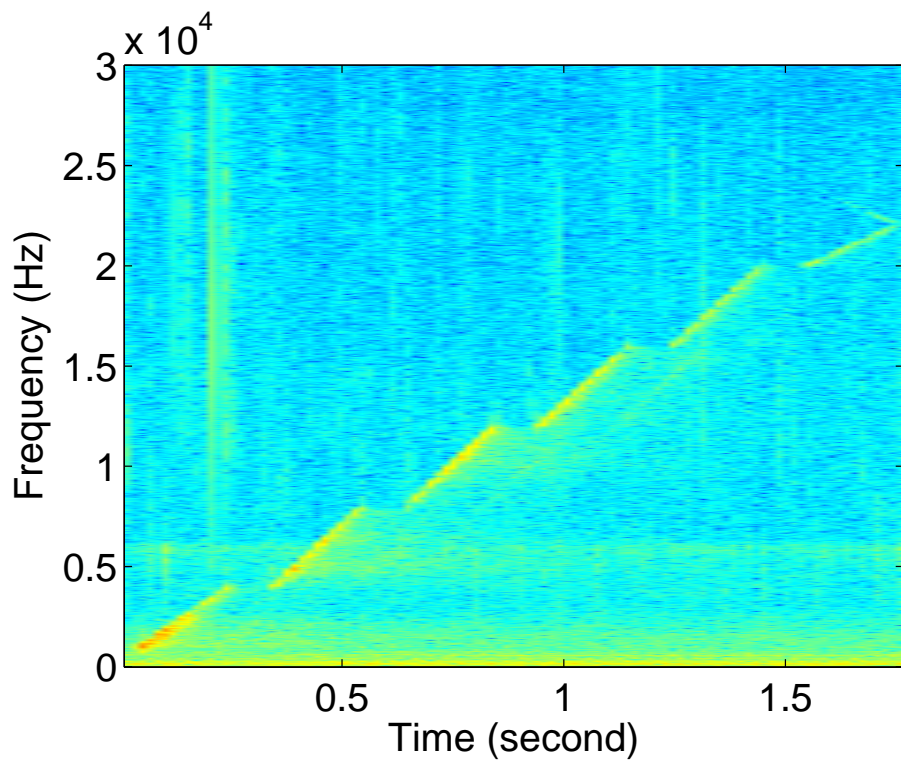
Figure 1.16: Spectrogram of received chirp signals B1-B6 from the 8th hydrophone (depth 11.12m) of the VLA16.

1.5.3   Channel Frequency Response

This section presents Frequency Response (FR) of the channel obtained using chirp signals. By using pulse compression method, we obtain Impulse Responses (IRs) of the channel for different bands by convolving the received signal with chirp signals, B1 to B6. Frequency responses associated with IRs at different bands are obtained by taking Fourier transforms of the IRs. Channel FRs obtained from the 8th hydrophone of the VLA16 at the beginning of pier and boat P2P transmissions are shown in Figure 1.17. Moreover, Figure 1.17 present the channel FRs obtained from the 4th hydrophone of the VLA8 at the beginning of S1-S4 P2P transmissions. We observe that there are some nulls in the responses caused by the underwater channel environment for all cases. Moreover, the amplitudes of the responses are higher at lower frequency band. Also, in general for all bands, the amplitudes of the responses for the pier P2P configuration are lower than those of other P2P configurations. This is may due to the fact that the range between source and the VLA is larger than other P2P cases and the transmission power is lower.

(a) Frequency response for pier case   (b) Frequency response for boat case

(c) Frequency response for S1 case   (d) Frequency response for S2 case

(e) Frequency response for S3 case   (f) Frequency response for S4 case

Figure 1.17: Frequency Responses at the 8th hyd. (11.12m depth) of the VLA16 for pier and boat cases, and at the 4th hyd. (30.9m depth) of the VLA8 for S1-S4 cases.

1.5.4   Channel simulator

This section presents channel impulse responses generated by the channel simulator developed at the University of Algarve based on Bellhop channel model (available at the UAN website, i.e. http://www.ua-net.eu/projects/simulator/). The inputs for the channel simulation are bathymetry of the experimental area as 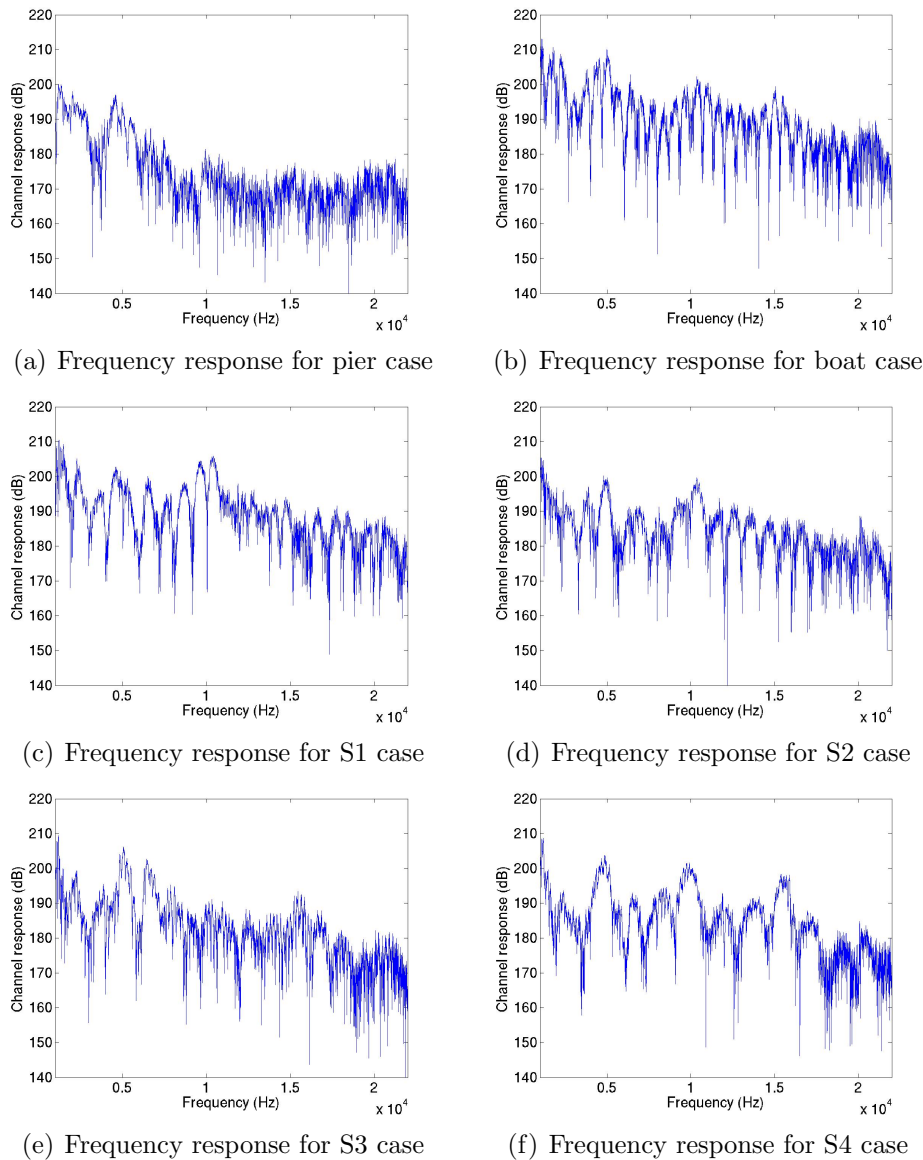shown in Figure 1.1, SSP, a baseband input signal, carrier frequency and sampling frequency. Moreover, source and the hydrophone array depths, as well as their location are required. Based on the report [3], the seafloors at the depth 0-10 m, 10-35m, and 35m on are calcareous rock, sand with posidonia prairies and occasional rocks/boulders, and sand with occasional rocks/boulders, respectively. In the simulator we consider the seafloor to be sand with the following bottom properties, the compressional speed of 1650 m/s, density of 1.9 g/cm3 and attenuation of 0.8 dB/wavelength [4, pp. 38].

For the pier P2P communications from the source to the VLA16, conducted on Sept 11, 2010, since there is no record of SSP at the experiment time (20:00 GMT), we use the SSP recorded Sept 12, 2010 at 14.59 GMT as shown in Figure 1.9-(a). The range between the source and the VLA16 is 836m. The IRs is simulated for the C2 signals with carrier frequency, fc of 10 kHz. The estimated IRs are obtained also from pulse compression method on the transmitted M-sequence. Figure 1.18 presents the amplitude of the simulated and estimated baseband IRs as functions of delay time and depths of the array of hydrophones. We observe that the arrival pattern between the simulated and estimated IRs is moderately agreeable.

In case of the rubber boat P2P communications between the source and the VLA16, conducted on Sept 13, 2010, we use the SSP measured at 7:24 GMT as shown in Figure 1.9-(b). The range between the source and the VLA16 is 127.38m. The IRs is simulated for the C3 signals with carrier frequency, fc of 15 kHz. The estimated IRs are also obtained from pulse compression method on the transmitted M-sequence. Figure 1.19 presents the amplitude of the simulated and estimated baseband IRs. We observe that the arrival pattern between the simulated and estimated IRs is in a good agreement.
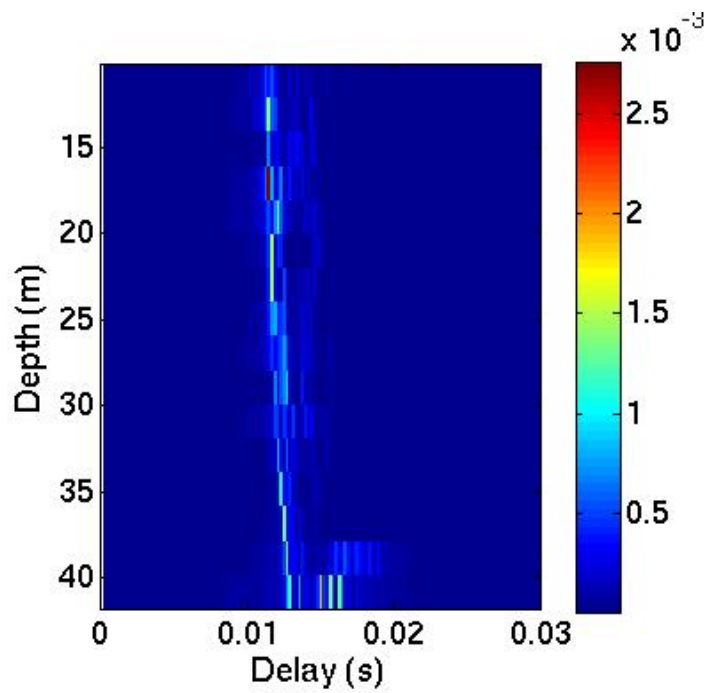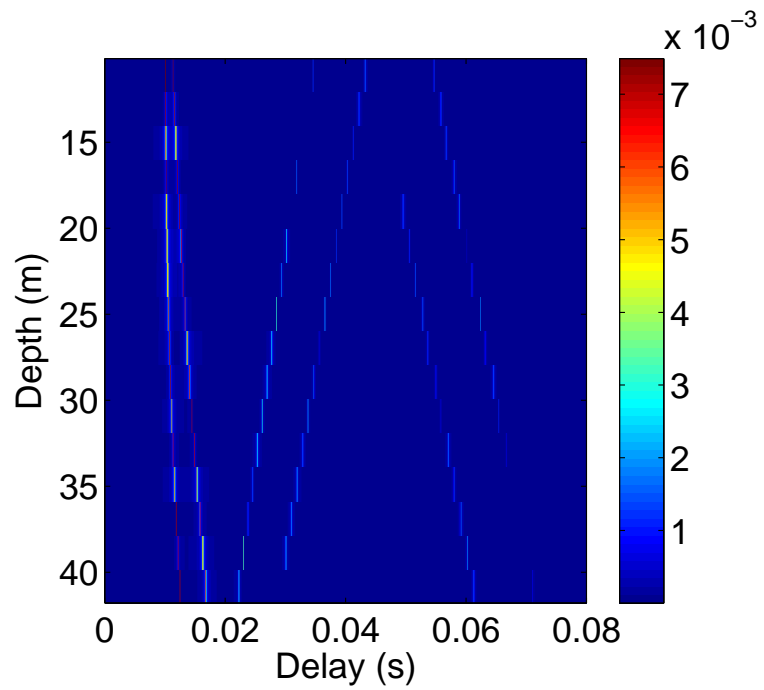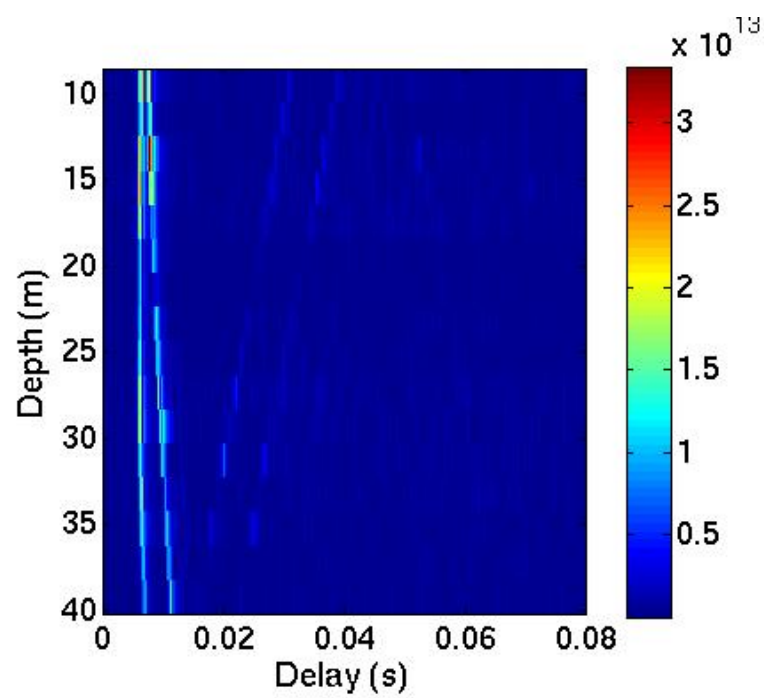
(a) Simulated IRs
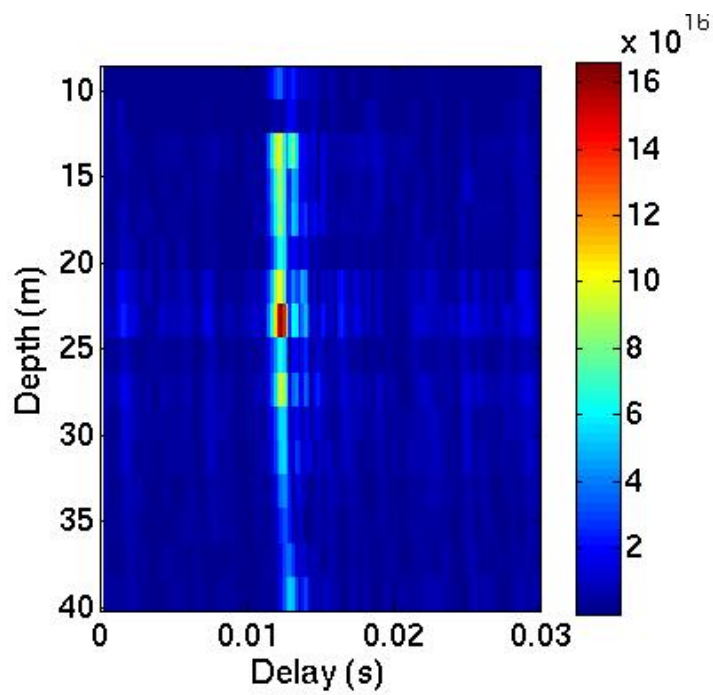
(b) Estimated IR

Figure 1.18: Simulated and estimated channel impulse responses for C2 pier case.

(a) Simulated IRs

(b) Estimated IR

Figure 1.19: Simulated and estimated channel impulse responses for C3 boat case.

1.5.5 Equalization results

In this work, we use three techniques for data processing, namely the combined pTR with an equalizer (e.g. Linear Equalizer (LE) and Decision Feedback Equalizer (DFE)), denoted by pTR-E and a variant of Frequency Shifted pTR with an equalizer [1], denoted by FSpTR-E, and MultiChannel equalizer MC-E [5].

This section presents the MSE and BER performance of the pTR-E, FSpTR-E, and MC-E schemes using the data from P2P communications, i.e. from the pier, boat and S1-S4 to the VLA. Note that the 16-hydrophone VLA was used in the pier and boat cases, while 8-hydrophone VLA was used in the S1-S4 cases. Since the 8th hydrophone of the 8-channel VLA shown in Figure 1.4 was not responsive or the data acquisition for this channel was failed, hence there are only 7 channels in data processing for S1-S4 cases.

In the following, we list common parameters used in all equalizers, where the notations are defined in [1]. Information data is BPSK modulated and transmitted at rates of 600, 1200, 2400, and 4800 sym/s for C1 to C4, respectively. In the first order PLL, the loop gain $G = 0.05$ is used, while the forgetting factor $\lambda = 0.995$ is employed for the RLS algorithm. A slot duration of $T_0 = 1$s is used for frequency shift decision making and $T_0 = 0.05$s is considered in the Doppler frequency estimation. We consider a set of candidate frequency shifts $\mathcal{F} = \{-300, -275, ..., 275, 300\}$, the threshold for frequency jump $\eta_f = 300$ Hz and that for normalized energy $\eta_E = 0.6$. Moreover, in discrete-time signals $L = 4$ samples per symbol is considered. For pTR-E and FSpTR-E, only a training sequence of length 200 symbols (the first 200 symbols of the data with structure presented in Table 1.3) is required for C1-C3 signals. For C4 signal, 200 training symbols are required at the beginning of every second in the 20s frame (discussed later in this section). Here, we account for the training symbols used only in data processing, i.e. for frame, symbol and phase synchronizations, and the symbol-spaced LE and DFE, while assuming that channel IRs can be estimated from other means, such as using M-sequence or chirp signals. Note that in this work we use M-sequences of length 63, 127, 255, and 511 symbols for C1 to C4 channel IR estimations, respectively. In the adaptive LE, 20 feedforward coefficients consisting of 10 causal and 10 anticausal coefficients are used, while in the DFE addition 10 feedback coefficients are used. For MC-E, the same number of feedforward and feedback coefficients as in the pTR-E and FSpTR-E are adopted. In the MC-E scheme, the frame synchronization and Doppler estimation are performed on each channel separately, and at least 1000 training symbols are required. For MC-E with C1 and C2 signals, a training sequence of 1000 symbols are used in all P2P cases, while for C3 and C4 signals, training sequences of length 1500 and 4000 symbols are used, respectively. We consider the decision directed mode of operation for the pTR-E, FSpTR-E and MC-E, where only a training sequence is required at the beginning of the transmission, unless state otherwise.

Table 1.6 presents the Signal plus Noise to Noise Ratio (SNNR) in dB. To calculate the SNNR from the real signals, the power of received signal in the band during data transmission frame is calculated and considered as the signal pulse noise power, while the noise power is calculated by the power of received signal in the band at time adjacent to the data transmission frame, where data signal was not transmitted. Then, the SNNR is the signal pulse noise power to noise power ratio.

We observe that the SNNR for pier P2P case is generally lower than other cases, this is in part due to the a longer range between source and receiver for this case, as documented in Table 1.1. Moreover, the SNNR is highest for C1 and decreases as we progress from C2 to C4. This is may due to the fact that a transmission loss increases with respect to frequency. Hence, C1 with $fc = 5$kHz obtains a larger SNNR than C4 with $fc = 19.6$kHz.

Therefore, this can also be responsible for the lower SNNR for higher band signals.

Table 1.6: Signal plus Noise to Noise Ratio (SNNR) in dB

Case	C1	C2	C3	C4
Pier	12.95	11.99	1.52	0.64
Boat	26.64	22.50	17.35	12.94
S1	28.08	17.79	11.34	3.48
S2	23.60	20.57	10.89	4.28
S3	26.00	9.29	11.33	4.14
S4	27.61	25.25	15.8	4.18

Table 1.7 summarizes the MSE and BER performance of the pTR-E, FSpTR-E, and MC-E schemes for C1 signal for all P2P configurations, i.e. from the pier, the boat and Leonardo at S1-S4. Except for the pier case, the pTR-E, FSpTR-E and MC-E schemes perform considerably well with MSE < -15 dB for all cases. Also, an error-free communication is obtained for all techniques for all cases, except the pier case. For the pier case, the performance of all schemes is poor, this is due to the fact that the range is larger and the SNNR is lower, than other cases. Moreover, the MC-E outperforms the pTR-E and FSpTR-E in terms of MSE for boat, S1 and S2 cases, while for pier, S3 and S4 cases the pTR-based schemes provide a slightly superior performance. Furthermore, all schemes with DFE perform at least as good as those with LE. Moreover, there is no significant gain when the FSpTR-E is used over the pTR-E when there is no relative movement between source and the VLA.

Table 1.7: BER and MSE performance of pTR-Equalizer for C1 signals.

Case	Eq. Type	pTR-E		FSpTR-E		MC-E	
		MSE (dB)	BER (%)	MSE (dB)	BER (%)	MSE (dB)	BER (%)
Pier	LE	-12.7	0.07	-12.5	0.1	-12	0.028
	DFE	-13.2	0.08	-13	0.22	-12.3	0.065
Boat	LE	-22.8	0	-22.6	0	-25.2	0
	DFE	-22.8	0	-22.8	0	-25.3	0
S1	LE	-15.1	0	-15.1	0	-17.0	0
	DFE	-16.5	0	-16.5	0	-17.4	0
S2	LE	-15.4	0	-16.7	0	-20.3	0
	DFE	-18.5	0	-18.4	0	-20.4	0
S3	LE	-17.1	0	-17.1	0	-16.6	0
	DFE	-17.8	0	-17.8	0	-16.9	0
S4	LE	-19.3	0	-19.2	0	-19.1	0
	DFE	-19.6	0	-19.6	0	-19.1	0

To explain the results of the pTR-based algorithms, we consider the temporal coherence of channel IRs with respect to probe IRs as in [6], where the coherence is defined to be the maximum cross-correlation between two signals normalized by the product of the square root of maximum autocorrelation of each signals. Here, we consider two sets of IRs, one is the array of probe IRs and another is that of IRs during data transmission. The cross-correlation and autocorrelation used in the coherence calculation are defined as the sum over individual cross-correlations and autocorrelations, respectively. We estimate the IRs
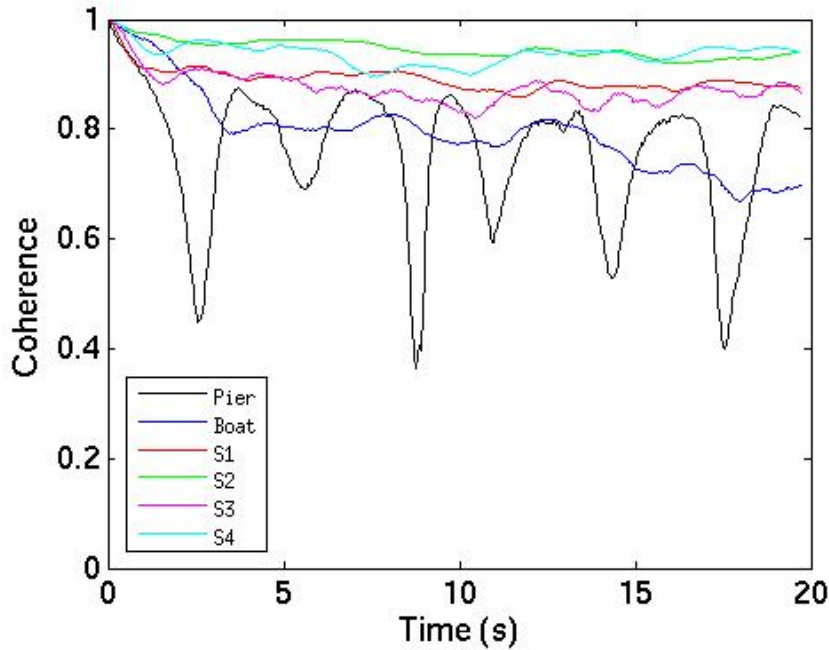
Figure 1.20: Temporal coherence for C1 case

during data transmission using RLS algorithm with the forgetting factor of 0.999 based on known transmitted sequence and received signals.

Figure 1.20 presents the temporal coherence between sets of IRs during 20s transmission with those of probe IRs for all C1 P2P cases. The results show that the coherence times (defined as the time that the coherence decays to $e^{-1} \approx 0.37$ [6]) are greater than 20s for all cases. Note, however, that for the pier case the coherence swings over time with periods where the coherence is lower than other cases. This could be the cause for poorer performance of the pier case as compared to other cases.

Table 1.8: BER and MSE performance of pTR-Equalizer for C2 signals.

Case	Eq. Type	pTR-E		FSpTR-E		MC-E	
		MSE (dB)	BER (%)	MSE (dB)	BER (%)	MSE (dB)	BER (%)
Pier	LE	-16.7	0	-16.3	0	-16.7	0.009
	DFE	-17.2	0	-16.7	0	-17	0.009
Boat	LE	-15.2	0	-15.4	0	-25.4	0
	DFE	-22.5	0	-22.5	0	-25.5	0
S1	LE	-8.2	0	-9.7	0	-16	0
	DFE	-10.8	0	-11.7	0	-16.3	0
S2	LE	-11.6	0	-12	0	-18.9	0
	DFE	-14.9	0	-14.9	0	-19.4	0
S3	LE	-5	2.4	-6.2	1.1	2.97 (-5.2)[1]	49.7 (1.8)[1]
	DFE	-4	4.9	-4.9	2.7	2.38 (0.89)[1]	50 (28.8)[1]
S4	LE	-18.5	0	-18.5	0	-19.2	0
	DFE	-19.4	0	-19.4	0	-19.5	0

Table 1.8 summarizes the MSE and BER performance of the pTR-E, FSpTR-E, and MC-E schemes for C2 signal for all P2P cases. Except for S3 case, the pTR-E and FSpTR-E schemes perform considerably well with MSE < -9 dB, and an error-free communication

---

[2]with a training sequence of length 1500 symbols

is obtained. Moreover, the MC-E can significantly outperform the pTR-E and FSpTR-E in terms of both MSE and BER for boat, S1 and S2 cases. The poor pTR-based performance for the C3 case maybe due to the low SNNR as presented in Table 1.6. Furthermore, we observe that the DFE provides a gain in performance over the LE when the error rate is low since, all schemes operate in decision directed mode, where the previous decisions are used in the equalization process. In the S3 case, where the BER is high, the schemes with DFE actually perform worse than those with LE, where there is no decision feedback used in the equalization. Moreover, for the S3 case, the MC-E provides a poor performance, this is in part due to the fact that 1000-symbol training sequence is insufficient for frame synchronization, i.e. the MC-E is more sensitive to synchronization problem than the pTR-based schemes that use only 200 symbols for such tasks. By using a training of length 1500 symbols, the results of MC-E scheme for S3 case are reported in parenthesis. Note that in this report, there is no attempt to optimize the equalizer parameters for each specific case.
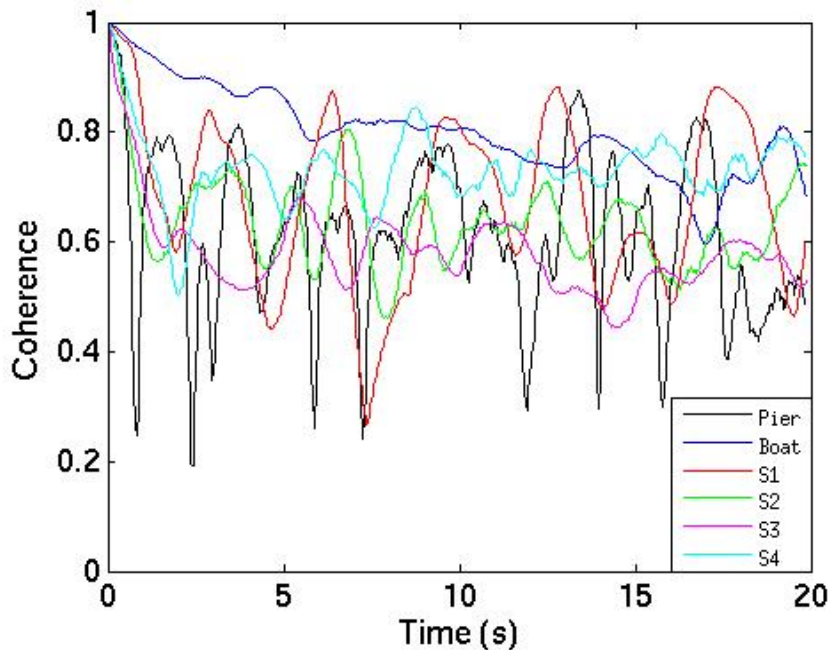

Figure 1.21: Temporal coherence for C2 case

Figure 1.21 presents the temporal coherence between sets of IRs during 20s transmission with those of probe IRs for all C2 P2P cases. The results show that there are high fluctuations in temporal coherence for all cases and overall coherence is lower than that associated with C1 signals as shown in Figure 1.20.

For C3 signals over all P2P cases, Table 1.9 summarizes the MSE and BER performance of the pTR-E, FSpTR-E, and MC-E schemes. For the pier P2P case, due to a weak transmission signal, a larger range from the VLA as compared to other cases, as well as a larger attenuation for high frequency signals, the SNNR of received signals are low (signals buried in noise) as reported in Table 1.6. With such low SNNR, the detection and synchronization are not possible, and the data recovery can not be done. Hence, we do not report the performance of all equalization schemes for this C3 signal. Similar observations are applied to the C4 signal. For this data set, the training sequences of length 1500 and 200 symbols are used for the MC-E, and pTR-based techniques, respectively.

Figure 1.22 illustrates the temporal coherence for all C3 P2P cases. We also observe high fluctuations in temporal coherence for all cases and overall coherence is lower than

Table 1.9: BER and MSE performance of pTR-Equalizer for C3 signals.

Case	Eq. Type	pTR-E		FSpTR-E		MC-E	
		MSE (dB)	BER (%)	MSE (dB)	BER (%)	MSE (dB)	BER (%)
Pier	LE	-	-	-	-	-	-
	DFE	-	-	-	-	-	-
Boat	LE	-8.9	0.3	-12.3	0	-20.3	0
	DFE	-10.3	0.18	-13.7	0	-20.5	0
S1	LE	-5.1	1.61	-5.0	1.83	-8.6	0.1
	DFE	-7.6	0.21	-7.5	0.24	-10.4	0.07
S2	LE	-8.7	0.11	-9	0.072	-9.9	0.061
	DFE	-9.7	0.033	-10	0.05	-10.5	0.044
S3	LE	-8.8	0.061	-8.7	0.14	-12	0.011
	DFE	-10.2	0.018	-10.1	0.026	-12.6	0.011
S4	LE	-8.5	0.059	-9.3	0.048	-16	0.015
	DFE	-11.0	0.0088	-11.9	0.0066	-16.3	0.022

that associated with C1 and C2 signals as shown in Figures 1.20 and 1.21.

The rubber boat case provides a superior performance than other cases, this is due to the fact that the 16 channel received signals were used in data processing, while for S1-S4 cases only 7 channel signals were used. Also, we observe that the FSpTR-E provides a considerable performance gain only in the rubber boat case, where there is a relative movement between the source and the receiver due to a strong current as shown in Figure 1.6. The boat movement implies a range change, where by applying proper frequency shifts to estimate IRs in pTR processing such change can be compensated [7] and the results illustrated this fact are shown in Figure 1.23. In static cases as in S1-S4, we observe that the FSpTR-E does not provide a considerably gain over the pTR-E. Furthermore, note that for S4 case, the MC-E technique with DFE provides lower MSEs, but with higher BERs than those of the pTR-based techniques. It is possible to obtain such results since the relationship between MSE and BER is nonlinear.

Table 1.10 summarizes the MSE and BER performance of the pTR-E, FSpTR-E, and MC-E schemes for C4 signals over all P2P cases. With pTR-E and FSpTR-E schemes, we apply a block-based processing, where the 20s frame is divided into 20 subframes of 1s duration each, and the pTR-E and FSpTR-E processings are applied to each subframe separately. The block-based processing is used in this data set because the channel IRs change rapidly (as shown by the rapidly decreasing temporal coherence in Figure 1.24), requiring a periodically channel IR estimation, rather than using only IR estimated at the beginning of the 20s frame for pTR processing. For MC-E, the training sequence of 4000 symbols is required. In this data set, overall performance of all schemes are poorer than other data sets, i.e. C1-C3. This is due to the low SNNR referred to Table 1.6 and a rapid channel variations as shown in Figure 1.24 by a low temporal coherence.

From Figures 1.20, 1.21, 1.22 and 1.24, we observe that C1 cases obtain a high temporal coherence and on average the coherence decreases as we progress from C1 to C4. This is due to the fact that channel IRs associated with higher frequency signals change rapidly over time as they are more prone to environmental changes.

With IRs estimated using received and transmitted signals, Figure 1.25 illustrates temporal coherence on every second within 20s frame for C4 case. The results show that the channel IRs for C4 case loose temporal coherence rapidly, and time coherence is much shorter than 1s.
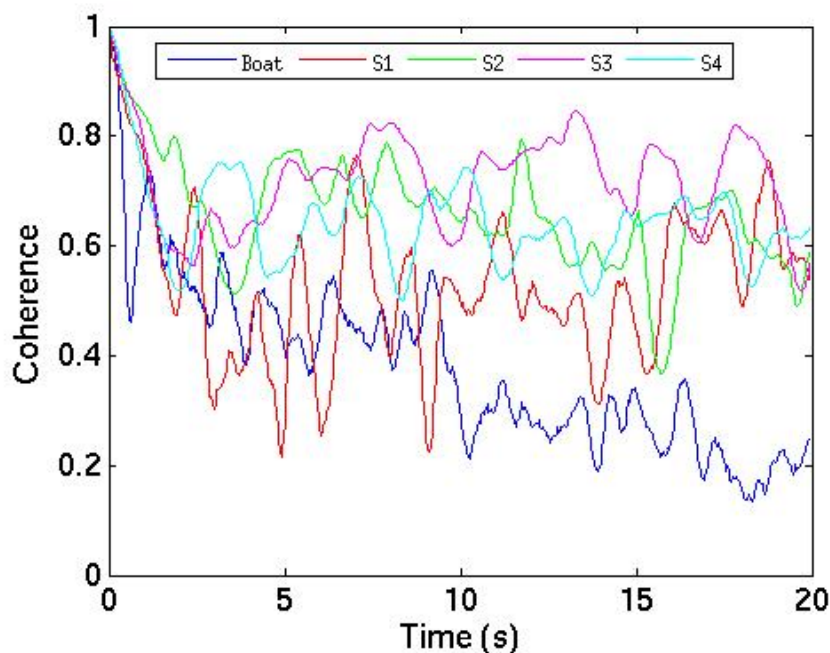
Figure 1.22: Temporal coherence for C3 case

Table 1.11 summarizes the required training symbols and obtained data throughput of pTR-E/FSpTR-E and MC-E schemes for C1 to C4 cases. With 200 training symbols per 20s frame required for pTR-based schemes as compared to 1000, 1000, and 1500 symbols required for MC-E scheme in C1, C2 and C3 cases, the pTR-E and FSpTR-E provide higher throughputs than the MC-E scheme. For C4 case, since 200 symbols are required every second for pTR-based scheme and 4000 symbols are required for the MC-E scheme, the same throughput is obtained for both pTR-based and MC-E schemes.

1.6   Conclusion

This report discusses the P2P communication experiments in the UAN2010 sea trial at Pianosa island, in Italy during September 7-25, 2010. The experiments were conducted at the north eastern area of the island. In the P2P experiments, the acoustic source transmitted various signals from UAN partners, i.e. CINTAL, ISME and FOI to the Vertical Array (VLA) of hydrophones. The received signals were acquired by Subsurface Telemetry Unit (STU) and sent back to the shore lab for data processing via a fiber optic cable. There were three sets of P2P communication experiments, where the source was placed at various locations, 1. from the Pianosa's pier, 2. from the rubber boat, moving due to a strong current, and 3. from stationary Leonardo, the NURC vessel at range-dependent bathymetry points. This report also presents the descriptions of the transmitted signals, in terms of frequency bands, data rate, bandwidth, etc. For CINTAL signals, four BPSK modulated signals, C1-C4 signals were transmitted, each with different data rates and frequency bands. Moreover, the data analysis, including spectrograms of both transmitted and received signals, as well as frequency responses of the channels at different bands are presented. For data demodulation, three techniques are used, i.e. the combined pTR with an equalizer, Frequency Shifted pTR with an equalizer and MultiChannel equalizer. For C1-C3, with data rates of 600, 1200 and 2400 symb/s, respectively, all three techniques provide an encouraging results, with error-free
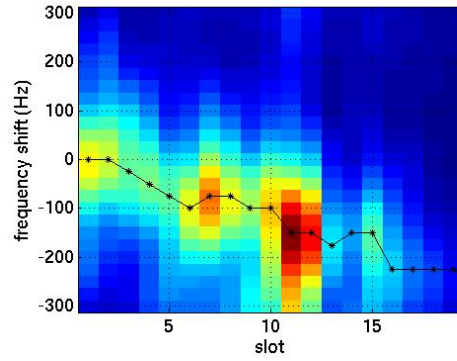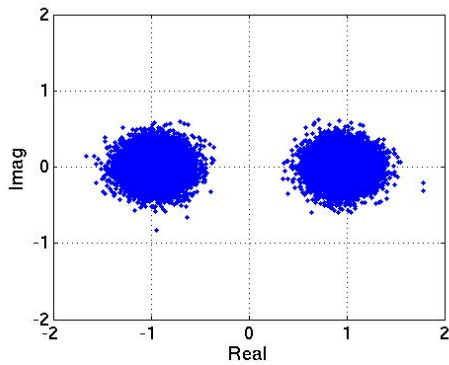
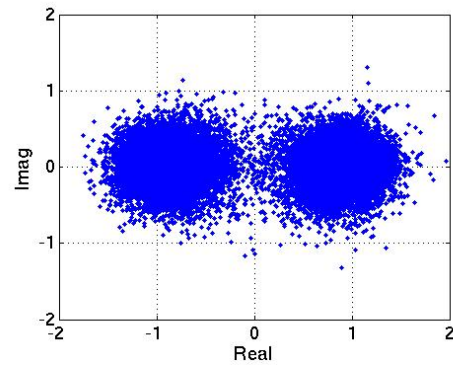(a) Received energy according to frequency shifts
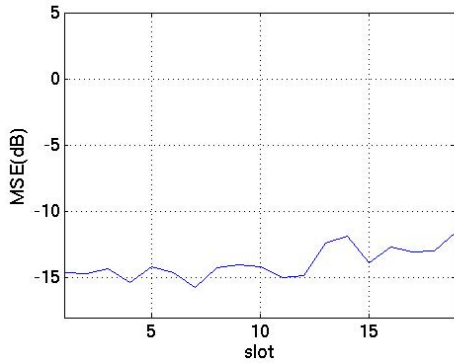
(b) MSE FSpTR-DFE
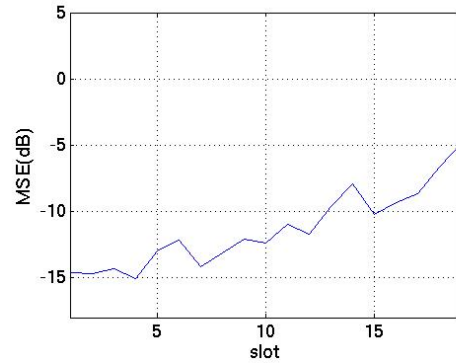
(c) MSE pTR-DFE

(d) Demodulated BPSK constellation for FSpTR-DFE

(e) Demodulated BPSK constellation for pTR-DFE

Figure 1.23: Performance comparison of pTR-DFE and FSpTR-DFE scheme for the rubber boat P2P case.
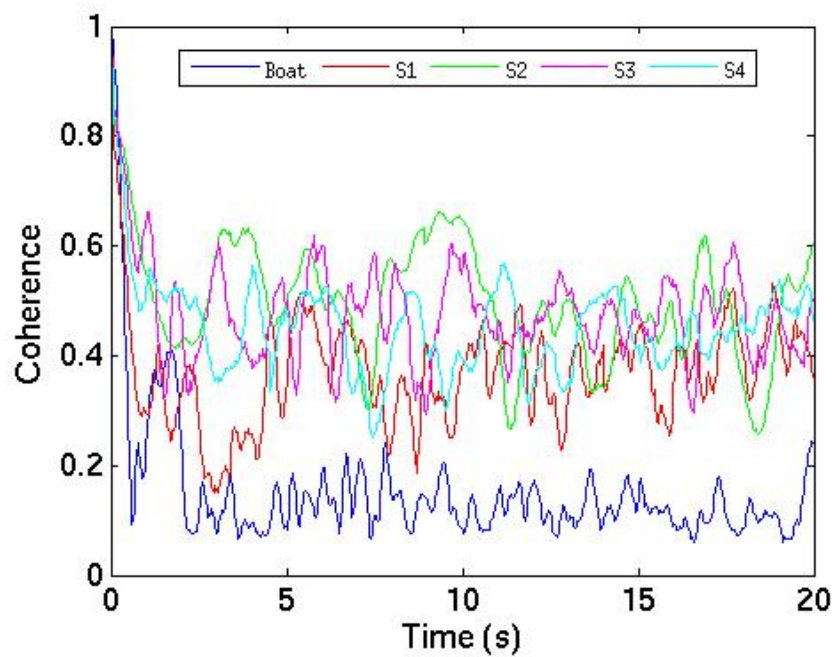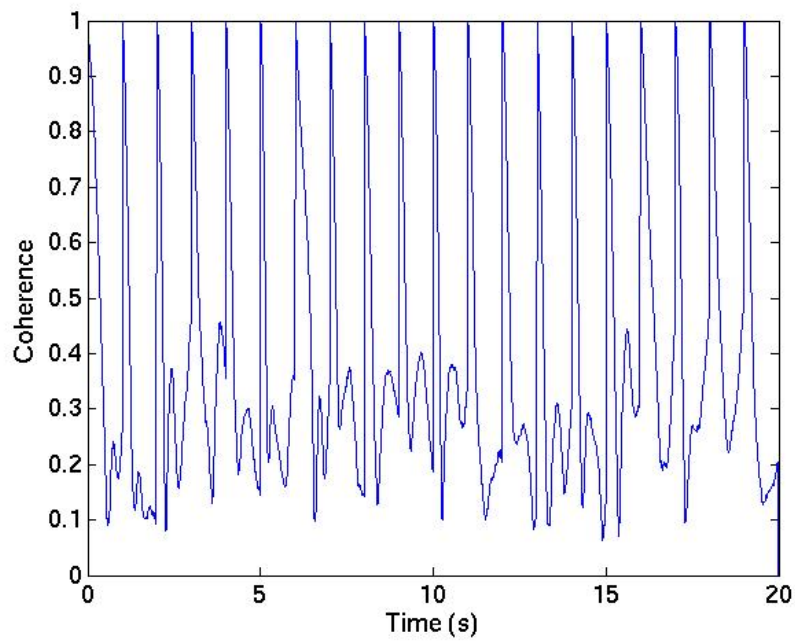
Figure 1.24: Temporal coherence for C4 case

Figure 1.25: Temporal coherence for C4 case

Table 1.10: BER and MSE performance of pTR-Equalizer for C4 signals.

Case	Eq. Type	pTR-E		FSpTR-E		MC-E	
		MSE (dB)	BER (%)	MSE (dB)	BER (%)	MSE (dB)	BER (%)
Pier	LE	-	-	-	-	-	-
	DFE	-	-	-	-	-	-
Boat	LE	-8.20	0.57	-8.46	0.5	-13.8	0.006
	DFE	-8.26	1.06	-8.87	1.08	-13.9	0.006
S1	LE	-4.8	2.98	-4.74	3.18	-5.8	0.9
	DFE	-4.89	3.0	-4.84	3.15	-6.2	0.8
S2	LE	-5.46	2.41	-5.44	2.45	-7.1	0.5
	DFE	-5.36	2.99	-5.43	2.71	-7.5	0.43
S3	LE	-5.08	2.46	-5.20	2.40	-4.9	2.4
	DFE	-5.27	2.33	-5.36	2.14	-4.5	4.1
S4	LE	-2.92	8.35	-2.97	8.12	-4	3.4
	DFE	-1.37	14.66	-1.09	16.10	3.9	66

Table 1.11: Data throughput

Case	Tx rate (sym/s)	Pilot (sym/frame)		Throughput (sym/s)	
		pTR-E & FSpTR-E	MC-E	pTR-E & FSpTR-E	MC-E
C1	600	200	1000	590	550
C2	1200	200	1000	1190	1150
C3	2400	200	1500	2390	2325
C4	4800	4000	4000	4600	4600

transmissions in most P2P cases for C1 and C2 signals. The MC-E provides a better performance than pTR-based techniques, but requires a longer training sequence and is more complex and more sensitive to synchronization problem. For C4 signals with data rate of 4800 symb/s and carrier frequency of 19.6 kHz, the performance of all equalizers is rather poor as compared to the C1-C3 signals due to low SNNR and temporal coherence.

With UAN2010 P2P experiments, the following objectives are fulfilled, 1. the P2P communications of data rate upto 2400 symb/s can be achieved using 16-hydrophone VLA, and 2. the current deployed techniques perform well for signals with data rate upto 2400 symb/s. However, the improvement on the techniques in the second objective should be developed for higher data rate by incoperating adaptive channel estimations to provide up-to-date IRs that can resolve the low coherence problem. Moreover, the development/improvement based on the current FSpTR-E scheme to adapt to environmental changes, such as changes due to surface waves, will be considered for future work.

Chapter 2

Appendix A

This appendix describes received signals, environmental data and matlab scripts given in the attached DVDs. The following filename structure is used to name received signal files, $STU0 - X_1X_2X_3Y_1Y_2Y_3Y_4Y_5Y_6.mat$, where $X_1X_2X_3$ represents a Julian day of the current year 2010, and $Y_1Y_2Y_3Y_4Y_5Y_6$ provides information of GMT time in Y_1Y_2, Y_3Y_4, and Y_5Y_6 in hour, minute and second, respectively.

Table 2.1 presents received signal filenames associated with P2P communications. Note that the indicative filename provides the information for the time at the beginning of the transmission (which last about 4:30 minutes).

Table 2.1: Filenames associated with P2P communications

Case	$X_1X_2X_3$	$Y_1Y_2Y_3Y_4Y_5Y_6$					
		F1	F2	F3	F4	F5	F6
Pier	254	200056	200556	201055	201723	-	-
Rubber boat	256	073606	074035	074633	075900	-	-
S1	263	122912	123510	124039	124509	125006	125537
S2	263	131504	132003	132503	133131	133629	134128
S3	263	135838	140337	140835	141334	141833	142331
S4	263	144027	145024	145554	150052	150621	151119
S1 repeat	263	153443	153943	154441	154910	155409	155838

Table 2.2 lists the directory names and their descriptions in the attached DVDs.

Table 2.2: DVDs data directories

Directory	Description
PierTX_20100911_MAT	Received signals for pier P2P communications
RHIB_TX_20100913_MAT	Received signals for boat P2P communications
Data_20100920_MAT	Received signals for S1-S4 P2P communications
Env_Data	Environmental data including sound speed profile, bathymetry, source depth, and boat GPS
Signal_Gen	Matlab files used to generate tone, chirp and C1-C4 signals

Bibliography

[1] U.Vilaipornsawai, A. Silva, and S.M. Jesus, "Combined adaptive time reversal and DFE technique for time-varying underwater communications," *Proc. European Conference on Underwater Acoustics (ECUA'10)*, July 2010.

[2] CINTAL, "WP4 deliverable 4.2 engineering test report," March 2010.

[3] A. Caiti, "Test-plan September 2010 experimental activities," August 2010.

[4] F.B. Jensen, W.A. Kuperman, M.B. Porter, and H. Schmidt, *Computational Ocean Acoustics*. Springer-Verlag, 2000.

[5] M. Stojanovic, J.A. Catipovic and J.G. Proakis, "Adaptive multichannel combining and equalization for underwater acoustic communications," *J. Acoust. Soc. Am.*, vol. 94, pp. 1621–1631, Sep. 1993.

[6] T. Yang, "Temporal resolution of time-reversal and passive-phase conjugation for underwater acoustic communications," *IEEE J. Ocean Eng.*, vol. 28, no. 2, pp. 229–245, April 2003.

[7] A. Silva, "Environmental based underwater communications," Ph.D. dissertation, University of Algarve, 2009.